

# Simulating Ion Transport and its Effects in Silicon Carbide Power MOSFET Gate Oxides

Daniel B. Habersat and Aivars J. Leļis

Power Components Branch,  
U.S. Army Research Laboratory  
Adelphi, MD 20852, USA

Email: daniel.b.habersat.civ@mail.mil

Neil Goldsman

Department of Electrical and Computer Engineering,  
University of Maryland  
College Park, MD 20742, USA

**Abstract**— A time domain, drift-diffusion based numerical simulator has been developed to better understand the influence of mobile ion transport in gate oxides for SiC power MOSFETs. Experimental evidence of mobile ion contamination in SiC MOS has been well documented in general, but proper analysis has been hampered by the presence of significant numbers of defects that distort the results. We report here on the initial results from a numerical simulator that will be able to incorporate models for these additional defect mechanisms in order to provide insight on these key mechanisms that are limiting the performance and reliability of SiC MOS technologies.

**Keywords**—metal oxide semiconductor (MOS); Silicon Carbide (SiC); Silicon Dioxide (SiO<sub>2</sub>); drift-diffusion; numerical simulation; mobile ions

## I. INTRODUCTION

Next-generation power devices, based on wide-bandgap semiconductors that can be operated at high temperatures and large power densities, are necessary to meet performance and reliability goals for future power conditioning systems, ranging in applications from motor drives and electric vehicles to grid-level power transformers. Silicon Carbide (SiC) MOSFETs are being investigated as a very attractive candidate. However, the oxidation process is more complicated than Si, largely due to the presence of carbon and 4H polytype crystal structure, which when combined with the necessarily thick oxide for power devices, produces oxide defects that are a major obstacle to achieving the full performance of SiC power MOSFETs. These defects include significant numbers of interface traps and near-interface oxide traps [1]. Additionally, bias-temperature stresses (BTS) show evidence of mobile ion contamination in the gate oxide [2], corroborated by triangular voltage sweep (TVS) measurements to quantify the amount of charge [3]. Mobile ions may include traditional elements or carbon-related complexes [4] and are likely a result of the fabrication process for SiC MOS.

Deconvolving the different effects of various oxide defects through standard experimental means has proven challenging given the complex dependencies on bias, temperature, and time. Efforts have been made to simulate the effects of interface and oxide traps [5],[6], but they do not consider mobile ions in the calculations. Given the strong dependence of oxide trap charging on time, a time-dependent (TD) mobile ion model is necessary to study both effects when

simultaneously present. To better understand the influence of mobile oxide charge, we developed a numerical simulator that emulates diffusive and field driven transport of mobile impurity ions in the gate oxide of SiC power MOSFETs.

Previous efforts to model mobile ion distributions in MOS devices have focused on steady-state equilibrium conditions and typically produce simple analytic solutions [7], or only consider transient currents from step function biases [8]. However, they are generally unable to account for additional types of oxide charges and cannot adequately predict device characteristics throughout measurement sequences typically used to characterize MOSFETs. Our finite-difference time-domain approach calculates the ion current as well as the charge and potential variations in SiC MOS as it is subjected to a time-varying applied bias.

## II. SIMULATING MOBILE CHARGES IN MOS STRUCTURES

### A. Simulation Domain

To study the movement of mobile charges that may be present in SiC/SiO<sub>2</sub> gate oxides, we utilized a finite-difference time-domain approach to calculate ion currents as well as charge and potential variations as an MOS structure is subjected to a time-varying bias. A schematic of the system being modeled can be seen in Fig. 1. The material is oriented so that the semiconductor/oxide interface is at the origin, while the gate ohmic contact is at  $x = t_{ox}$ , the oxide thickness. The spacing between mesh points is allowed to be non-uniform and

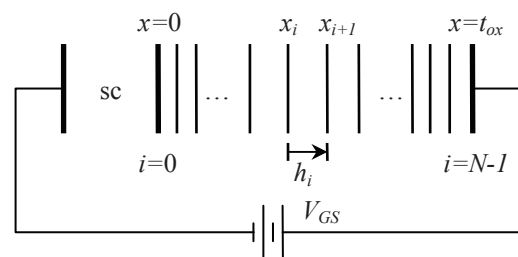


Fig. 1. Schematic of the simulation domain used in this work. The oxide is partitioned by a finite-difference mesh and oriented so that the semiconductor/oxide interface is located at the  $i = 0$  ( $x_0 = 0$ ) grid point, while the oxide's ohmic contact is at  $i = N - 1$  ( $x_{N-1} = t_{ox}$ ). Adjacent mesh points are separated by a distance  $h_i = x_{i+1} - x_i$ . An externally applied time-dependent bias  $V_{GS}(t)$  is placed across the structure.

defined as  $h_i = x_{i+1} - x_i$ . The index  $i$  is used to refer to a quantity when evaluated at that mesh point, while  $i + \frac{1}{2}$  refers to the value at the midpoint between  $i$  and  $i + 1$ .

A discussion of the application of the drift-diffusion equations for the simulation of charge transport in semiconductor materials can be found in [9], and general-purpose methods for multivariate root finding in [10]. The semiconductor region was not simulated, but instead calculated based on idealized relations derived in a manner similar to that in [11].

### B. Potential Variation

The first independent variable used in the simulation is the potential  $\psi_i$ , which is governed throughout the oxide by Poisson's equation

$$F_{\psi_i} = \frac{d^2\psi}{dx^2}\Big|_i + \frac{q}{\epsilon_{ox}}(p_i + C_i) = 0, \quad (1)$$

where  $\psi$  is the potential variable,  $q$  is the elementary charge constant,  $\epsilon_{ox}$  is the oxide permittivity,  $p_i$  is the mobile ion charge concentration, and  $C_i$  is any additional net space charge (such as fixed charges or charged oxide traps).

The boundary condition for  $\psi$  at the SiC/SiO<sub>2</sub> interface is

$$F_{\psi_0} = -\epsilon_{sc}E_s(\psi_0) - \epsilon_{ox}\frac{d\psi}{dx}\Big|_0 - Q_{it}(\psi_0) = 0 \quad (2)$$

where  $\epsilon_{sc}$  is the semiconductor permittivity,  $E_s(\psi)$  is the ideal semiconductor surface field, and  $Q_{it}(\psi)$  is the net interface trap charge present. Expressions for the surface field as a function of band bending are widely available (e.g., [11]). Interface trapped charge can either be ignored or calculated using an assumed distribution of interface traps such as in [5]. At the ohmic contact, the boundary condition is simply

$$F_{\psi_{N-1}} = \psi_{N-1} - V_{GS}(t) = 0. \quad (3)$$

### C. Ion Transport Model

The other independent variable used for simulation is the mobile ion potential  $\phi_{p_i}$ , which equates to the concentration  $p_i$  by the relation

$$p_i = e^{\phi_{p_i}/U_T}, \quad (4)$$

where  $U_T$  is the thermal voltage. This potential representation allows the simulation variables to be similarly scaled and is like the often used quasi-Fermi representation for semiconductor carriers but without the  $\psi$ -dependence.

For this work, mobile ion transport is modeled as the standard drift-diffusion current that arises from the presence of electric fields and concentration gradients. The time-dependent continuity equation is thus

$$F_{p_i} = \frac{dJ_p}{dx}\Big|_i + q\frac{dp_i}{dt} + qR_i = 0, \quad (5)$$

where  $J_p$  is the mobile ion current defined as

$$J_p\Big|_{i+\frac{1}{2}} = -q\left[\mu_p p \frac{d\psi}{dx} + D_p \frac{dp}{dx}\right]_{i+\frac{1}{2}}, \quad (6)$$

$R$  is the net recombination-generation term,  $\mu_p$  is the ionic mobility and  $D_p$  is ionic diffusivity. Ions present in the gate oxide are assumed to be positively charged; slight modification to the signs in (5) and (6) are necessary for negatively charged ions.

In general, the recombination term  $R_i$  will be zero. It could, however, be used to model additional effects such as electron-ion exchange [12] or ion trap "hopping" [13]. As in other studies of mobile ion transport, mobility and diffusivity are assumed to be connected by the Einstein relation ( $D = U_T\mu$ ). By dropping the  $dp_i/dt$  term above, (5) becomes the time-independent continuity equation (which can be used for finding the initial state or simulating quasi-static measurement techniques such as triangular voltage sweep [3]).

The semiconductor interface and ohmic contact are assumed to be impermeable to mobile ions. The technique of mirror imaging can be used to ensure no flow of ions:

$$J_p\Big|_i = J_p\Big|_{i+\frac{1}{2}} - J_p\Big|_{i-\frac{1}{2}} = 0, \quad (7)$$

when substituted into (5), gives the boundary condition.

### D. Conservation of Charge

When dealing with mobile ions, unlike with electrons and holes in a semiconductor, the total number of charges present must be conserved. This introduces an additional constraint on the simulation, in the form of

$$F_N = \int_0^{t_{ox}} p(x)dx - N_p = 0 \quad (8)$$

where  $N_p$  is the total ion count and is an input to the simulation. This integral will need to be numerically calculated based on the charge densities at each mesh point.

As detailed in [9], carrier densities cannot reasonably be assumed to follow a linear distribution between mesh points, and in fact calculating the total or net effective ionic charge with a simple summation as in [14] would introduce unacceptable error into the calculations, particularly as the local field in the oxide increases. To calculate the integral, we split the integral into sections between adjacent mesh points and utilize the carrier growth functions developed for holes (i.e., positively charged carriers). The working assumptions made to use this method for electrons and holes should also apply to mobile ions if they obey the same basic drift-diffusion mechanics. The discretized form of the integral then becomes

$$\begin{aligned} \int_0^{t_{ox}} p(x)dx &= \sum_{i=0}^{i=N-2} \int_{x_i}^{x_{i+1}} p(x)dx \\ &= \sum_{i=0}^{i=N-2} \int_{x_i}^{x_{i+1}} [p_i(1 - g_i(x)) + p_{i+1}g_i(x)]dx \end{aligned} \quad (9)$$

where the carrier growth function  $g_i(x)$  is defined by [9] as

$$g_i(x) = \begin{cases} \frac{1 - \exp\left(v_i \frac{x - x_i}{h_i}\right)}{1 - e^{v_i}} & v_i \neq 0 \\ \frac{x - x_i}{h_i} & v_i = 0 \end{cases} \quad (10)$$

and  $v_i = (\psi_{i+1} - \psi_i)/U_T$ .  $g_i(x)$  can be analytically integrated and evaluated over each mesh interval. That expression is found to be

$$I_i = \int_{x_i}^{x_{i+1}} g_i(x) dx = h_i \begin{cases} \frac{1}{1 - e^{-v_i}} - \frac{1}{v_i} & v_i \neq 0 \\ \frac{1}{2} & v_i = 0 \end{cases}. \quad (11)$$

Combining (9), (10), and (11), (8) can now be expressed in its final discretized form to conserve the total number of mobile ions,

$$F_N = \sum_{i=0}^{i=N-2} p_i(h_i - I_i) + p_{i+1}I_i - N_p = 0. \quad (12)$$

The addition of a constraint on the global charge amount makes the system of equations overdetermined (for  $N$  mesh points, there will be  $2N$  variables when solving for  $\psi_i$  and  $\phi_{p_i}$  but  $2N + 1$  equations). However, the boundary requirements for ion impermeability at the domain edges are Neumann-type and this allows the system to remain consistent and uniquely solvable.

If ions were allowed to either become spatially trapped in a localized potential well or change net charge state, then these quantities would need to be tracked separately and the total of all ion states then conserved.

### III. RESULTS

#### A. Quasi-Static Conditions

##### 1) Equilibrium Charge Distributions

To verify that the simulator was fundamentally sound, we used it to calculate the equilibrium distributions of positively-charged mobile ions in an ideal oxide structure as a function of applied field ( $\mathcal{E} = V_{GS}/t_{ox}$ ), which are shown in Fig. 2. These

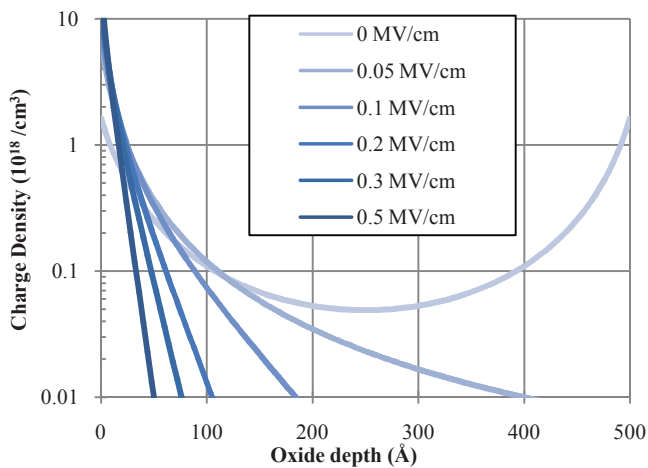


Fig. 2. Equilibrium charge distributions in an SiO<sub>2</sub> oxide for different applied fields. Reversed fields are symmetric about the middle of the oxide and were excluded for clarity. Total charge density  $N_p = 10^{12} \text{ cm}^{-2}$ .

calculations require the use of the time-independent form of (5). The device is a basic oxide with two ohmic contacts and no semiconducting region, 500 Å thick and at a temperature of 150 °C. With no applied bias, the charge distribution is symmetric; as the applied bias is increased, the positive charges are repelled from the high bias side and pile up on the other end. Even under small fields, the equilibrium charge distributions become highly asymmetric and consist of essentially all of the charge moved to one side or the other. The resulting charge distributions are consistent with those found elsewhere via other methods [7].

##### 2) Triangular Voltage Sweep

Fig. 3 shows both the experimentally measured and numerically simulated gate currents of a SiC MOS capacitor during a triangular voltage sweep measurement. The capacitor was p-type doped to around  $10^{16} \text{ cm}^{-3}$  and had an oxide thickness of about 500 Å. From the TVS measurement performed at 150 °C, total mobile ion density was estimated to be  $N_p \cong 1.2 \times 10^{12} \text{ cm}^{-2}$ . Even when a simple simulation is performed that includes no additional effects (such as interface or oxide traps), basic agreement is obtained although the experimental data is broader and shows additional features.

Although Si MOS devices are routinely characterized for mobile ion contamination around 150°C, SiC has a much larger bandgap than Si and will retain extrinsic doping at this temperature. This complicates the analysis as the change in surface charge density from sweeping the device through accumulation to inversion introduces a non-negligible current that must be accounted for. Since SiC MOS devices have a well-known BTS-induced instability that significantly worsens as temperatures are increased, elevating the temperature further to increase the intrinsic carrier concentration is not an acceptable solution. Additionally, a time-dependent activation of additional charge traps during BTS has been shown [15] which may pose problems for TVS measurements that necessarily require a long and slow gate bias ramp at elevated temperature. Given the nature of these challenges, numeric device simulation may present the best results for accurate mobile ion extraction.

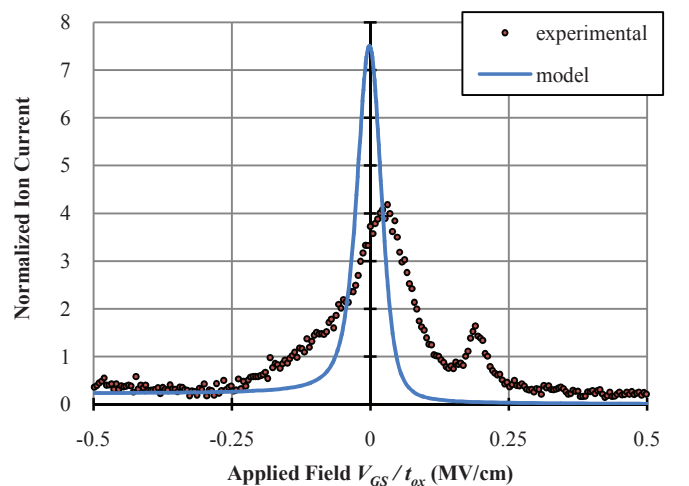


Fig. 3. Triangular voltage sweep measurement (dots) and simulation (line) data of a SiC MOS capacitor at 150°C. Area under the curve is total ion density,  $N_p \cong 1.2 \times 10^{12} \text{ cm}^{-2}$ .

### B. Transient Conditions

The time-dependent continuity equation (5) can be used to study how a charge distribution at equilibrium reacts to an abrupt change in bias, simulating a BTS. The simulation of a 500 Å SiO<sub>2</sub> oxide at a temperature of 150 °C with a 10<sup>12</sup> cm<sup>-2</sup> density of ions of mobility of 10<sup>-13</sup> cm<sup>2</sup>/V s, subjected to an abrupt change in applied bias from +1 V to -1 V, is shown in Fig. 4. Time slices of the distribution of mobile ions in the oxide are shown from the moment before the bias step to until the charges have reached a new equilibrium state.

The redistribution of charges moves the position of the charge centroid, which determines the net voltage shift of the device's terminal characteristics. Fig. 5 shows how the charge centroid evolves during the initial stages of a typical BTS applied to a SiC MOS device; the ionic current induced by the movement in this charge distribution is also shown. The simulated device in this case is an ideal 500 Å oxide experiencing an abrupt bias stress of ±3 MV/cm at 150 °C; the mobile ion population consists of 10<sup>12</sup> cm<sup>-2</sup> positive charges with a mobility of 10<sup>-12</sup> cm<sup>2</sup>/V s.

The analytic transit time ( $t_t = t_{ox}/\mu\mathcal{E}$ ) for these conditions is 1.67 s, which agrees well with the model predictions of 2-3 s for the centroid position to stabilize and ionic current to go to zero. Interestingly, the transient ionic current is relatively insensitive to time until the final portion of the movement and could (in this case) be reasonably approximated by a step function located at the transit time.

### REFERENCES

[1] K. Matocha and V. Tilak, "Understanding the inversion-layer properties of the 4H-SiC/SiO<sub>2</sub> interface," *Mater. Sci. Forum*, vol. 679-680, pp. 318-325, March 2011.  
 [2] A.J. Lelis, D. Habersat, R. Green, and N. Goldsman, "Temperature-dependence of SiC MOSFET threshold-voltage instability," *Mater. Sci. Forum*, vol. 600-603, pp. 807-810, September 2008.

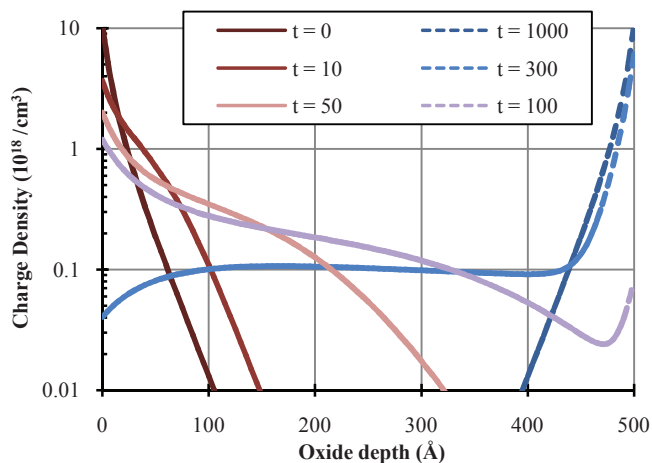


Fig. 4. Time-dependent movement of a 10<sup>12</sup> cm<sup>-2</sup> mobile ion population in 500 Å of SiO<sub>2</sub> following an abrupt switch from +1 V to -1 V applied bias. The charge distribution at various time steps is shown, and basically moves from left to right as time increases.  $\mu = 10^{-13}$  cm<sup>2</sup>/V s,  $T = 150$  °C, and time from start  $t$  is in seconds.

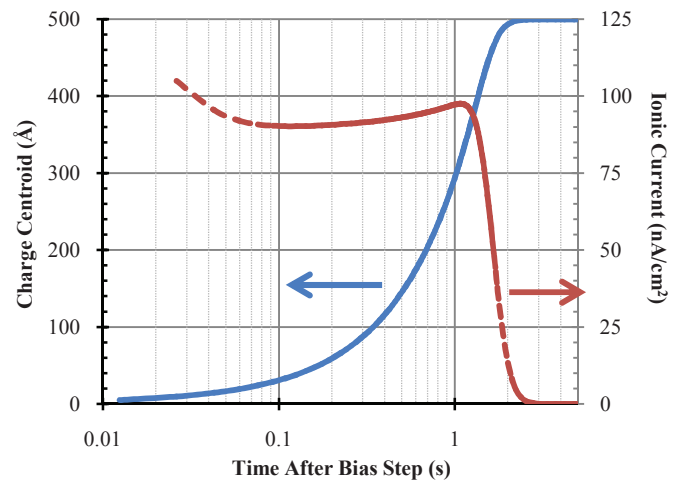


Fig. 5. Plot of the charge centroid (solid, left axis) and ionic current (dashed, right axis) versus time after an abrupt switch from -15 V to +15 V for a 10<sup>12</sup> cm<sup>-2</sup> mobile ion population in 500 Å-thick SiO<sub>2</sub> ( $\mu = 10^{-12}$  cm<sup>2</sup>/Vs,  $T = 150$  °C).

[3] D.B. Habersat, A.J. Lelis, and R. Green, "Detection of mobile ions in the presence of charge trapping in SiC MOS devices," *Mater. Sci. Forum*, vol. 717-720, pp. 461-464, May 2012.  
 [4] A. Chanthaphan et al., "Investigation of unusual mobile ion effects in thermally grown SiO<sub>2</sub> on 4H-SiC(0001) at high temperatures," *Appl. Phys. Lett.*, vol. 100, pp. 252103, June 2012.  
 [5] S. Potbhare et al., "A physical model of high temperature 4H-SiC MOSFETs," *IEEE Trans. Elec. Dev.*, vol. 55, pp. 2029-2040, August 2008.  
 [6] A.J. Lelis, D.B. Habersat, R. Green, and N. Goldsman, "Two-way tunneling model of oxide trap charging and discharging in SiC MOSFETs," *Mater. Sci. Forum*, vol. 717-720, pp. 465-468, May 2012.  
 [7] V. Mitra, H. Bentarzi, R. Bouderbala, and A. Benfdila, "A theoretical model for the density distribution of mobile ions in the oxide of metal-oxide-semiconductor structures," *J. Appl. Phys.*, vol. 73, pp. 4287-4291, May 1993.  
 [8] G. Greeum and B.J. Hoenders, "Theoretical solution of the transient current equation for mobile ions in a dielectric film under the influence of a constant electric field," *J. Appl. Phys.*, vol. 55, pp. 3371-3375, May 1984.  
 [9] S. Selberherr, *Analysis and Simulation of Semiconductor Devices*. Wien, Austria: Springer-Verlag, 1984.  
 [10] J.E. Dennis, Jr. and R.B. Schnabel. *Numerical Methods for Unconstrained Optimization and Nonlinear Equations*. Englewood Cliffs, NJ: Prentice-Hall, 1983.  
 [11] E.H. Nicollian and J.R. Brews, *MOS (Metal Oxide Semiconductor) Physics and Technology*. New York, New York: John Wiley & Sons, 1982.  
 [12] E.I. Goldman, A.G. Zhdan, and G.V. Chucheva, "Ion transport phenomena in oxide layer on the silicon surface and electron-ion exchange effects at the SiO<sub>2</sub>/Si interface," *J. Appl. Phys.*, vol. 89, pp. 130-145, January 2001.  
 [13] M. Iwamoto, "Transient current across insulating films with long-range movements of charge carriers," *J. Appl. Phys.*, vol. 79, pp. 7936-7943, May 1996.  
 [14] K. Yamashita, M. Iwamoto, and T. Hino, "Thermally stimulated current properties of mobile ion in SiO<sub>2</sub> film of MOS structure and its numerical analysis," *Jpn. J. Appl. Phys.*, vol. 20, pp. 1429-1434, August 1981.  
 [15] R.Green, A.Lelis, D.Habersat, and M.El, "Investigation of a high temperature oxide-trap activation model for SiC power MOSFETs," in *Proc. Int Semiconductor Device Research Symp. (ISDRS)*, Dec. 7-9, 2011, pp. 1-2.